Pramana – J. Phys. (2017) 89:11
DOI 10.1007/s12043-017-1399-7

Density functional study of $AgScO_2$: Electronic and optical properties

K C BHAMU[1,*], JAGRATI SAHARIYA[2], RISHI VYAS[3] and K R PRIOLKAR[1]

[1]Department of Physics, Goa University, Taleigao Plateau, Goa 403 206, India
[2]Department of Physics, Manipal University, Jaipur 303 007, India
[3]Department of Physics, Swami Keshvanand Insitute of Technology, Management and Gramothan, Jaipur 302 017, India
*Corresponding author. E-mail: kcbhamu85@gmail.com

Published online 20 June 2017

Abstract. This paper focusses on the electronic and optical properties of scandium-based silver delafossite ($AgScO_2$) semiconductor. The density functional theory (DFT) in the framework of full potential linearized augmented plane wave (FP-LAPW) scheme has been used for the present calculations with local density approximation (LDA) and generalized gradient approximation (GGA). Electronic properties deal with energy bands and density of states (DOSs), while optical properties describe refractive index and absorption coefficient. The energy bands are interpreted in terms of DOSs. The computed value of band gap is in agreement with that reported in the literature. Our results predict $AgScO_2$ as indirect band-gap semiconductor. Our calculated value of the refractive index in zero frequency limits is 2.42. The absorption coefficient predicts the applicability of $AgScO_2$ in solar cells and flat panel liquid crystal display as a transparent top window layer.

Keywords. Density functional theory; band structure; optical properties.

PACS Nos 71.15.Mb; 71.20.−b; 78.20.−e

1. Introduction

The wide band-gap delafossites have emerged as a new family of transition metal oxide materials with a number of remarkable electronic and optical properties [1–4]. Among them, copper and silver-based delafossites are of particular interest because they have sufficiently wide band gap and can be used as window layer in a variety of optical devices. The unique feature of this semiconductor family is that they can be combined with N-type semiconductor to form PN junction [1] which can be used as an inner layer of solar cells for electricity generation. This peculiar characteristic has established a benchmark in invisible electronics and opened a new era in solar cell technology [5–9].

Dietrich and Jansen [10] synthesized and reported the 3R phase of $AgScO_2$. Shannon *et al* [11] reported the syntheses of various delafossite families including $AgScO_2$ and provided lattice parameters for the 3R phase. These lattice parameters are converted into 2H-type structure and then optimized by Kandpal and Seshadri using the CASTEP code [12]. They reported the influence of d10–d10 interactions and predicted the candidature of these structures for transparent conducting oxide (TCO) applications. Nagarajan *et al* [13] synthesized a series of compounds like $CuMO_2$ (Sc, Y, Cr, $Fe_{0.5}V_{0.5}$) and $AgMO_2$ (M = In, Sc, Cr, Ga) and reported the conductivity of these compounds. They predicted that Cu-based compounds show higher conductivity than Ag-based compounds. Sheets *et al* [14] synthesized $AgScO_2$ and observed the mixed phase of this compound. They predicted the optical band gap for $AgScO_2$ to be 3.8 eV. They also reported theoretical band gap (2.4 eV) using LMTO method at gamma point of Brillouin zone (BZ) which is in far agreement with the said optical value. Using minima hopping method combined with high-throughput calculations Cerqueira *et al* [15] explored the periodic table in search of novel oxide phases and predicted structure as well as band gap for vaious oxide structures. Cerqueira *et al* [15] reported the band gap for $AgScO_2$ as 2.1 eV which was appreciablly smaller than the band gap calculated by Sheets *et al* [14]. The debate over band gap and limited number of reports encouraged the present investigation on optical and electronic properties of $AgScO_2$.

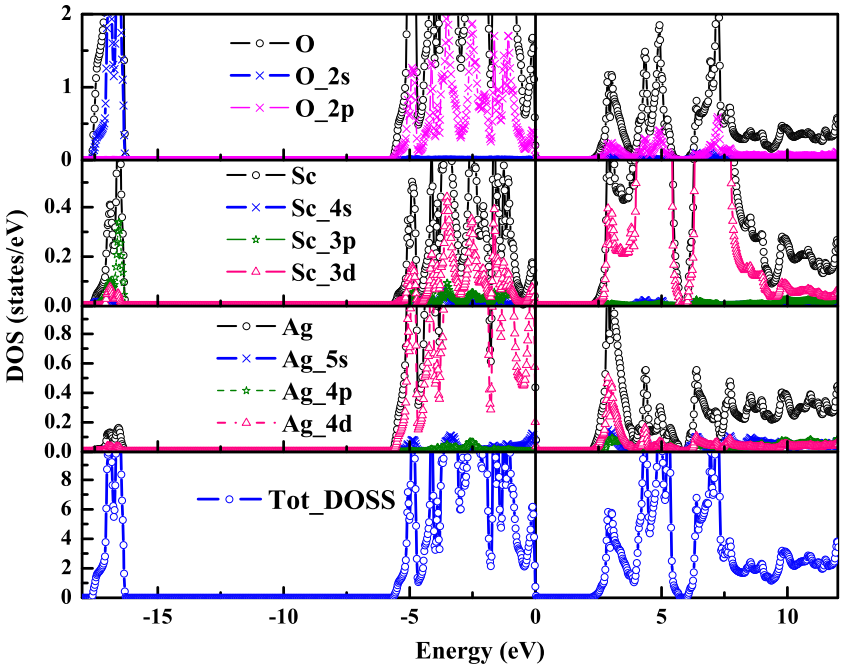

Figure 1. Density of states for 2H-$AgScO_2$.

The unit cell of $AgScO_2$ consists of linear AgO_2 dumb-bell structure linked with Sc-centred edge-centred octahedral structure in basal plane. In the ScO_6 octahedral layer, each Sc atom is coordinated by six O atoms, while each O atom is coordinated with three Sc atoms and one Ag atom. Depending on the stacking of O–Ag–O dumb-bell structure, the crystal can stabilize either in a rhombohedral (3R) or hexagonal (2H) symmetry. It is reiterated several times in the literature that the difference in the formation energy between these two structures is very less, and synthesized material may crystallize in either 3R or 2H structure [10,13,14,16].

2. Computational details

We have employed density functional theory (DFT) under full potential linearized augmented plane-wave (FP-LAPW) method as used in WIEN2K code [17]. In this approach, the unit cell is divided into two regions: non-overlapping spherical symmetric muffin-tin spheres and interstitial region. The potential in muffin-tin spheres is represented by spherical harmonics basis sets while for the interstitial region it is represented by plane-wave basis sets. To carry out the standard calculation, we fixed the cut-off parameter $R_{mt}K_{max}$ as 7 for the convergence of basis sets, G_{max} (Fourier expansion of potentials) is held at 12 a.u.$^{-1}$ in the interstitial region. The variable l_{max} for the spherical harmonic function is set to 10 which determines the behaviour of wave function inside the muffin-tin sphere. The self-consistent energy convergence criteria were kept fixed at 10^{-4} Ryd. The radius of the muffin-tin spheres (RMTs) for Ag, Sc and O are 2.07, 2.06 and 1.78 bohr, respectively.

3. Electronic properties

3.1 *DOSs and energy bands*

For the band-structure calculation, we have used local density approximation (LDA) and generalized gradient approximation (GGA). Except for some subtle structures and the band gap, the overall trends are similar, and so we report here only band structures computed by using GGA. The calculated band gap from LDA was 2.29 eV. Figure 1 represents the DOSs (energy bands) of 2H-$AgScO_2$ calculated using GGA.

From figure 1, we see that the bottom of the valence band region is mainly dominated by Sc(3p) and O(2s) states with a small contribution from Sc(3d) state. It results in the origin of energy bands in the bottom of the valence band between −17 eV and −16 eV in figure 2.

In the region just below the Fermi energy, the significant contribution is from Ag(3d) and O(2p) states with a small contribution from Sc(3d) states. This mixing of atomic orbitals is responsible for energy bands just below the Fermi energy level as shown in figure

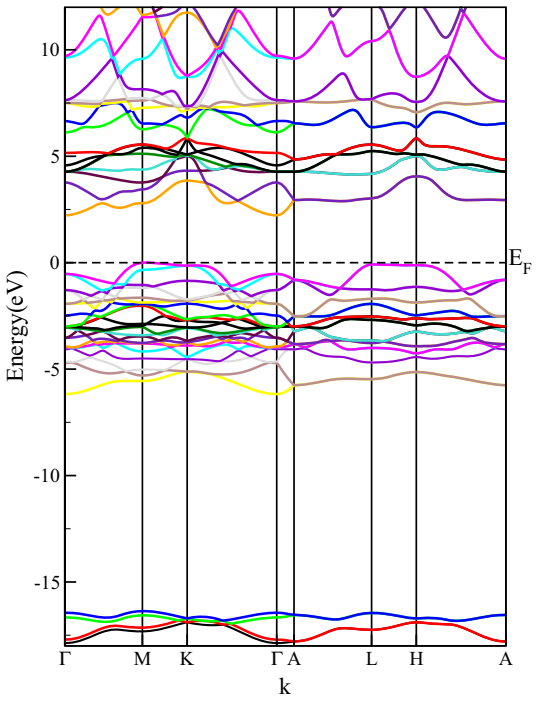

Figure 2. Energy bands for 2H-$AgScO_2$ along with high symmetric directions.

2 where bands are dispersed in the energy range from −6 eV to Fermi level. The empty region just above the Fermi level indicates that there is no orbital contribution which results in the band gap in this compound. In figure 2 this gap is 2.3 eV. In the upper region of the conduction band, overlapping occurs between Sc(3d) and O(2p) states which correspond to the origin of energy bands in the energy range above 2.3 eV. It can be seen from figure 2, that the valence band maximum and conduction band minimum are not on the same wave vector which predicts the indirect band gap nature of the present compound. This type of semiconducting nature is also reported by Sheets *et al* [14]. The calculated band gap is 2.8 eV which is in better agreement with the optically observed band gap (3.8 eV) in comparison to the band gap of 2.4 eV predicted by Sheets *et al* [14].

4. Optical properties

4.1 *Refractive index*

Figure 3 represents the refractive index for 2H-$AgScO_2$. We see from figure 3, that the overall shape of the perpendicular $[n^{\perp}(\omega)]$ and parallel $[n^{\parallel}(\omega)]$ components of refractive index is quite similar to a small shift in the energy of incident photons. In the inset of figure 3, we have shown the birefringence $\Delta n(\omega)$, the difference

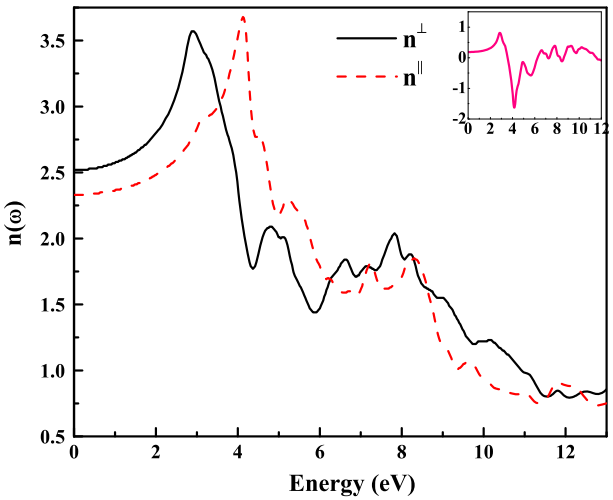

Figure 3. Refractive index for 2H-$AgScO_2$.

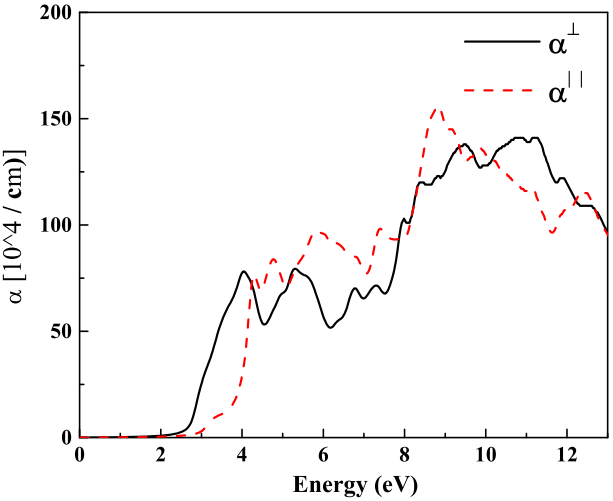

Figure 4. Absorption coefficient for 2H-$AgScO_2$.

between $[n^{\perp}(\omega)]$ and $[n^{\parallel}(\omega)]$ components. The $\Delta n(\omega)$ also trace back the nature of $[n^{\perp}(\omega)]$ and $[n^{\parallel}(\omega)]$ components which show the less anisotropic nature of the present compound. The value of $n^{\perp}(\omega)$, $n^{\parallel}(\omega)$ and $n(0)$ and components in zero frequency limit were found to be 2.51, 2.33 and 2.42, respectively, while the birefringence $\Delta n(\omega)$ is deduced to be 0.18. The positive value of the refractive index in the shown range, i.e. in the energy limit up to 13 eV, indicates that $AgScO_2$ remains linear to electromagnetic frequency.

4.2 *Absorption coefficient*

In figure 4, we present the absorption coefficient of the 2H-$AgScO_2$ compound. In the energy range between 0.0 eV and 2.8 eV, the absorption coefficient is almost zero, and hence there is lack of interaction between the incident photon and the medium. It is well known that

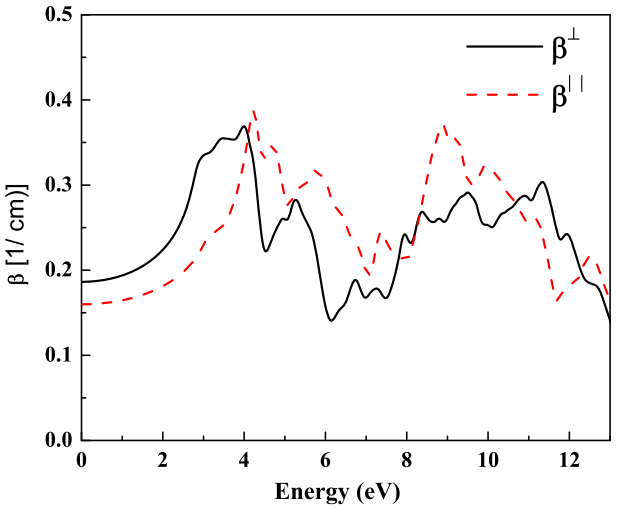

Figure 5. The reflectivity curve for 2H-$AgScO_2$.

this range of energy corresponds to infrared (1.24 meV–1.7 eV) and visible (1.7 eV–3.3 eV) region of the solar spectrum and lack of interaction between the incident radiation and the medium predicts that medium is transparent to the incident radiation in this range. As the energy of photons increase, the absorption coefficient starts increasing which shows an interaction between photons and atomic charge of the medium and hence trapping of photons in the medium. We can see that absorption coefficient increases almost linearly with the increase of incident photons energy, and reaches maximum up to energy around 11 eV. This energy range lies in the UV range of the solar spectrum and predicts that the medium absorbs maximum photons in the UV region. The transparency for the visible region of solar spectrum and absorbance of photons in the UV region makes it useful for flat panel displays and window layer in solar cells.

4.3 *Reflectivity*

To support the calculations for absorption coefficient of 2H-$AgScO_2$, reflectivity is plotted in figure 5 on an arbitrary scale. It is apparent from the reflectivity curve that in the energy range of 0.0 eV to 2.8 eV, the reflectivity of the incident photons is negligible in comparison to the absorption coefficient. The absorption coefficient is of the order of 10^4 while the reflectivity curve is of the order of 10^{-1}. This comparison between the absorption curve and the reflectivity curve in the range 0.0 eV–2.8 eV clearly indicates that the incident photon in this energy range mostly gets transmitted. A similar interpretation for the transparent nature of the TCOs in this energy range is also mentioned in refs [18–22].

5. Conclusions

We have computed energy bands and density of states for 2H-$AgScO_2$. Our results confirm the indirect band gap nature of this compound. Our computed band gap is in good agreement with the optically reported band gap. Our calculated refractive index and absorption coefficient suggest the applicability of 2H-$AgScO_2$ as a window layer in solar cells and flat panel displays.

Acknowledgements

The authors are grateful to Prof. P Blaha for providing the WIEN2K code. KCB acknowledges UGC, New Delhi (India) for the Dr D S Kothari Postdoctoral Fellowship [No. 4-2/2006(BSR)/PH/13-14/0113]. JS is thankful to SERB, New Delhi (India) for grant under Fast Track Young Scientist scheme (SR/FTP/PS-121/2012). The authors also acknowledge the computing resources provided by IUAC, New Delhi.

References

[1] H Kawazoe, M Yasukawa, H Hyodo, M Kurita, H Yanagi and H Hosono, *Nature* **389**, 939 (1997)
[2] H Yanagi, S Inoue, K Ueda, H Kawazoe, H Hosono and N Hamada, *J. Appl. Phys.* **88**, 4159 (2000)
[3] A N Banerjee, R Maity and K K Chattopadhyay, *Mater. Lett.* **58**(**1**), 10 (2004)
[4] Z Deng, X Zhu, R Tao, W Dong and X Fang, *Mater. Lett.* **61**, 686 (2007)
[5] R Hoffman and J Wager, US Patent No. 7,026,713 B2 (11 Apr. 2006)
[6] H Yanagi, K Ueda, H Ohta, M Orita, M Hirano and H Hosono, *Solid State Commun.* **121**, 15 (2001)
[7] K Tonooka, H Bando and Y Aiura, *Thin Solid Films* **445**, 327 (2003)
[8] K L Chopra, S Major and D K Pandya, *Thin Solid Films* **102**, 1 (1983)
[9] J Cai and H Gong, *J. Appl. Phys.* **98**, 033707 (2005)
[10] V Dietrich and M Jansen, *Z. Naturforsch. B* **66**, 227 (2011)
[11] R D Shannon, D B Rogers and C T Prewitt, *Inorg. Chem.* **10**, 713 (1971)
[12] H C Kandpal and R Seshadri, *Solid State Sci.* **4**, 1045 (2002)
[13] R Nagarajan, N Duan, M K Jayaraj, J Li, K A Vanaja, A Yokochi, A Draeseke, J Tate and A W Sleight, *Int. J. Inorg. Mater.* **3**, 65 (2001)
[14] W C Sheets, E S Stampler, M I Bertoni, M Sasaki, T J Marks, T O Mason and K R Poeppelmeier, *Inorg. Chem.* **47**, 2696 (2008)
[15] T F T Cerqueira, S Lin, M Amsler, S Goedecker, S Botti and M A L Marques, *Chem. Mater.* **27**, 4562 (2015)

[16] W C Sheets, E Mugnier, A Barnabe, T J Marks and K R Poeppelmeier, *Chem. Mater.* **18**, 7 (2006)
[17] P Blaha, K Schwarz, G K H Madsen, D Kvasnicka and J Luitz, An Augmented Plane Wave + Local Orbitals Program for Calculating Crystal Properties *WIEN2k_14.2* ISBN 3-9501031-1-2 (Techn. University at Wien, Austria 2014)
[18] M F Iozzi, P Vajeeston, R Vidya, P Ravindran and H Fjellvg, *RSC Adv.* **5**, 1366 (2015)
[19] M A Ali, Afzal Khan, S H Khan, T Ouahrani, G Murtaza, R Khenata and S B Omran, *Mater. Sci. Semicond. Process.* **38**, 57 (2015)
[20] X Nie, H S Wie and S B Zhang, *Phys. Rev. B* **65**, 075111 (2002)
[21] D O Scanlon and W Watson, *Chem. Mater.* **21**, 5435 (2009)
[22] K C Bhamu, R Khenata, S A Khan, M Singh and K R Priolkar, *J. Electron. Mater.* **45**, 615 (2016)